Biweekly and 21–30-Day Variations of the Subtropical Summer Monsoon Rainfall over the Lower Reach of the Yangtze River Basin

JING YANG

State Key Laboratory of Earth Surface Processes and Resource Ecology, Beijing Normal University, and State Key Laboratory of Numerical Modeling for Atmospheric Sciences and Geophysical Fluid Dynamics (LASG), Institute of Atmospheric Physics, Chinese Academy of Sciences, Beijing, China

BIN WANG

Department of Meteorology, and International Pacific Research Center, University of Hawaii at Manoa, Honolulu, Hawaii, and College of Physical Oceanography and Marine Environment, Ocean University of China, Qingdao, China

BIN WANG AND QING BAO

State Key Laboratory of Numerical Modeling for Atmospheric Sciences and Geophysical Fluid Dynamics (LASG), Institute of Atmospheric Physics, Chinese Academy of Sciences, Beijing, China

(Manuscript received 5 January 2009, in final form 26 September 2009)

ABSTRACT

The lower reach of the Yangtze River basin (LYRB) is located at the central region of the mei-yu and baiu front, which represents the subtropical East Asian (EA) summer monsoon. Based on the newly released daily rainfall data, two dominant intraseasonal variation (ISV) modes are identified over the LYRB during boreal summer (May–August), with spectral peaks occurring on day 15 (the biweekly mode) and day 24 (the 21–30-day mode). These two modes have comparable intensities, and together they account for above about 57% of the total intraseasonal variance. Both ISV modes exhibit baroclinic structures over the LYRB at their extreme phases.

However, the genesis and evolutions associated with the two modes are different. Considering the genesis of their extreme wet phases over the LYRB, the biweekly mode is initiated by a midlatitude jet stream vorticity anomaly moving southeastward, while the 21–30-day mode is primarily associated with a low-level westward propagation of an anticyclonic anomaly from 145° to 120°E, which reflects the westward extension of the western North Pacific subtropical high (WNPSH). The development of the biweekly mode at LYRB is enhanced by the northwestward movement of a low-level anticyclonic anomaly from the Philippine Sea to the south of Taiwan, which is a result of the enhancement of the WNPSH resulting from its merger with a transient midlatitude high. In contrast, the development of the 21–30-day mode is enhanced by an upper-level trough anomaly moving from Lake Baikal to far east Russia. These two ISV periodicities are also found to be embedded in their corresponding source regions.

The new knowledge on the sources and evolutions of the two major LYRB ISV modes provides empirical predictors for the intraseasonal variation in the subtropical EA summer monsoon.

1. Introduction

During boreal summer, from May to August, many flooding events over the Yangtze River basin (YRB) are associated with extremely active phases of the intraseasonal variation of the mei-yu (or baiu) front. For example, the severe flooding over the lower reach of the YRB (LYRB) in the summer of 1998 was associated with two intraseasonal wet events occurring in June and July (e.g., Zhu et al. 2003; Wang et al. 2003; H. Liu et al. 2008), and the heavy Yangtze rainfall during the summer of 1991 was also attributed to the atmospheric intraseasonal variability (e.g., Mao and Wu 2006).

Many previous studies of boreal summer intraseasonal variation (ISV) were focused on the tropical monsoon

Corresponding author address: Dr. Jing Yang, State Key Laboratory of Earth Surface Processes and Resource Ecology, Beijing Normal University, Beijing 100875, China.
E-mail: yangjing@bnu.edu.cn

DOI: 10.1175/2009JCLI3005.1

region. Two dominant ISV modes that were prevalent over South Asia and the tropical western North Pacific regions were found, namely, the northward-propagating 30–50-day mode (e.g., Krishnamurti and Subrahmanyam 1982; Chen and Murakami 1988; Hsu and Weng 2001; Kemball-Cook and Wang 2001; Lawrence and Webster 2002; Hsu et al. 2004) and the westward-propagating quasi-biweekly mode (e.g., Krishnamurti and Bhalme 1976; Krishnamurti and Ardanuy 1980; Chen and Chen 1995; Annamalai and Slingo 2001; Mao and Chan 2005; Kajikawa and Yasunari 2005; Yang et al. 2008).

In contrast to the tropical ISV, the preferred frequencies and properties of ISV in the subtropical East Asia (EA) summer monsoon region, such as LYRB, are quite different. Most previous studies have dealt with a single case or a small sample of cases. For instance, a 12–24-day oscillation was reported as prevailing over YRB during the 1989 summer (Chen et al. 2000), which was out of phase with that over the South China Sea (SCS). The strong signal of the 30–60-day oscillation was shown in the 1998 YRB flood (Zhu et al. 2003), which featured a northward propagation from the tropics. A 15–30-day periodicity was found to contribute to the 1991 summer Yangtze–Huaihe River basin flood, and was influenced by the penetration of both midlatitude perturbation and westward propagation of the anomalous subtropical western North Pacific high (Mao and Wu 2006). A quasi-biweekly oscillation has been reported over the lower reach of YRB during late summer in 1981 (Chao 1991) and early summer in 1991 (Zhang et al. 2002). Unfortunately, a generally accepted description of the dominant periodicities and major characteristics of the ISV over YRB has not emerged yet.

The present study attempts to give a comprehensive description of the ISV over the central region of the EA subtropical front, the LYRB, with a set of relatively long-record (1979–2002) daily rainfall observations and daily circulation made by reanalysis. This paper is organized as follows. Section 2 introduces datasets and methodology. The dominant ISV periodicities over the LYRB are given in section 3, and the structures and evolutions of the dominant ISV modes over the LYRB are depicted in section 4. Section 5 discusses the possible origins of the two ISV modes, and a summary is given in section 6.

2. Data and methodology

The daily precipitation data on land are compiled by the project entitled the ''Asian Precipitation–Highly-Resolved Observational Data Integration towards Evaluation of the Water Resources (APHRODITE),'' which is being conducted by the Research Institute for Humanity and Nature (RIHN) and the Meteorological Research Institute (MRI) of the Japan Meteorological Agency (JMA). The APHRODITE project has developed state-of-the-art daily precipitation datasets with high-resolution grids (0.5°) for Asia. The datasets are created primarily with the data obtained from a rain gauge observation network. The domain of the EA product (APHRODITE-EA) used in this study covers the area of 5°–55°N, 65°–155°E (Xie et al. 2007; Yatagai et al. 2008). The length of the data spans from 1979 to 2002. In addition, because of the unavailability of reliable daily rainfall in tropical regions for the 1979–2002 period, daily outgoing longwave radiation (OLR) from the National Oceanic and Atmospheric Administration (NOAA; Liebmann and Smith 1996) were used as a substitute of daily rainfall in the tropics.

Daily circulation data are extracted from the following reanalysis datasets: 1) the National Centers for Environmental Prediction (NCEP)/Department of Energy (DOE) Reanalysis 2 (NCEP-2), from 1979 to 2002 (Kanamitsu et al. 2002); 2) the 40-yr European Centre for Medium-Range Weather Forecasts (ECMWF) Re-Analysis (ERA-40), from 1979 to 2002 (Uppala et al. 2005); and 3) the Japanese 25-year Reanalysis Project (JRA-25), from 1979 to 2002 (Onogi et al. 2007). Sensitivity tests did not show much difference between the three reanalyses in their circulation fields associated with each dominant ISV mode. Therefore, in this paper, to avoid repetition we only show the results from ERA-40.

The ISV component was obtained from the ''raw'' daily precipitation time series through first removing climatology, and then removing synoptic fluctuations by taking a 5-day running mean. The climatology is represented by climatological 5-day running mean time series, which includes both the slow annual cycle (represented by the first three Fourier harmonics) and the climatological intraseasonal oscillation (CISO). Over the subtropical EA and the western North Pacific monsoon regions, CISO was found to be significant, which is an invariant portion of ISV from year to year (Nakazawa 1992; Wang and Xu 1997). In EA, the well-known northward seasonal advance of the subtropical rain belt (e.g., Tao and Chen 1987; Lau et al. 1988; Ding 1992; Kang et al. 1999) belongs to part of fast annual cycle (LinHo and Wang 2002) and can be represented best by CISO (Yang 2008; J. Liu et al. 2008). Quasi 60 days was the major periodicity of CISO over the subtropical EA region (Kang et al. 1999; Yang 2008). Therefore, the ISV component we will focus on in this study is the year-to-year varying part of the ISV.

To identify statistically significant and dominant periodicities, we apply the fast Fourier transform (FFT) method with a tapered window (Bingham et al. 1967),

which is one of the most common methods of spectral analysis, to the time series of ISV over a given location during a given season (May–August). In this study, the selection of the major periodicities is determined by calculating the average of individual power spectra for each of the 24 summer seasons (1979–2002) over the LYRB region. Statistical significance of power spectra was tested according to the method of Gilman et al. (1963) based on the power spectrum of mean red noise.

Because the filtered data involve high autocorrelations between consecutive daily values, the degree of freedom is much less than the original sample size. Using Chen's (1982) method, the effective degree of freedom was calculated for each variable at each grid within the Eurasian domain (0°–80°N, 40°–180°E) for each dominant ISV mode. For simplicity, for each ISV mode we used its smallest effective degree of freedom for each variable at every grid point for the statistically significant test (around 96 for the 21–30-day mode and 184 for the 10–20-day mode). With this effective degree of freedom, a *t* test is applied to obtain the confidence level of the correlation coefficient. In addition, the significance of the correlation coefficients was retested through the 1000-times Monte Carlo simulation procedure (Wilks 1995; Livezey and Chen 1983). In all cases studied here, we found that the confidence level determined by this Monte Carlo technique was much less than the correlation coefficient value obtained from the first method. Thus, in the following section, the confidence level of the correlation coefficient value is determined by a *t*-test statistic.

3. Dominant periodicities of ISV in the LYRB summer precipitation

To obtain the dominant periodicities of ISV over the LYRB (29°–34°N, 115°–120°E), we present a 24-summer-averaged (May–August) power spectra of the APHRODITE-EA rainfall ISV component in this region during the period from 1979 to 2002 (Fig. 1). In addition to the multiyear mean power spectra, Fig. 1 also shows the lines of red noise spectra, the 99% a priori and the 99% a posteriori confidence levels. Based on the 99% a priori confidence level, three frequency bands are identified over the LYRB during boreal summer, which occur, respectively, on days 10–20 (peaking on day 15; hereafter "biweekly"), days 21–30 (peaking on day 24), and days 7–9 (peaking on day 8). These three modes can be well separated based on a 99% a posterior confidence level.

We calculated the percentage variance of each major ISV mode against the total ISV. The contributions are, respectively, 22% from the 21–30-day mode, 35% from the biweekly mode, and only 6% from the 7–9-day mode.

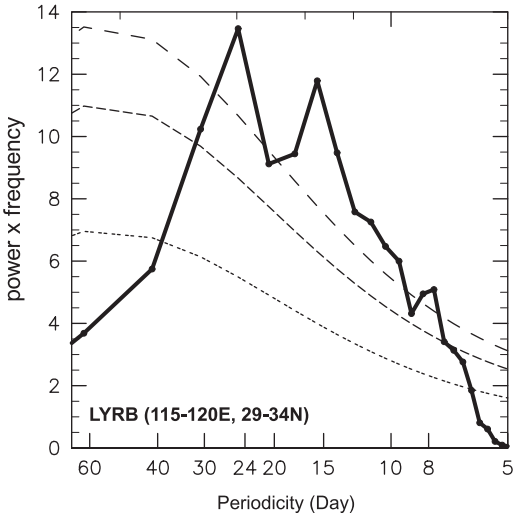

FIG. 1. Mean power spectra of the rainfall ISV component by calculating the average of the individual power spectra for each of the 24 summer seasons (1979–2002) over the LYRB region. Markov red noise spectrum (dotted line), a priori 99% confidence bound (dense dashed line), and a posterior 99% confidence level (sparse dashed line). The *x* abscissa has been rescaled into the natural logarithm of the frequency, and the corresponding *y* abscissa times frequency. The bandwidth is 0.0076.

Thereby, the biweekly and 21–30-day modes are considered to be the most important two ISV modes over the LYRB, with around a 57% contribution, which are the focuses in this study; the biweekly mode is the most significant. Note that the 30–60-day oscillation over the EASM region, which was studied in some previous studies, did not show up in the spectral analyses of the year-to-year varying intraseasonal oscillation, because it largely belongs to the CISO associated with normal annual advance of the subtropical monsoon front (see section 2 for data treatment).

The daily time series of the total ISV are checked year by year. The threshold to select the significant ISV event is defined as 1.5 times the standard deviation of the total ISV during boreal summer over the LYRB domain. If the absolute value of the maximum (minimum) intensity in its wet (dry) phase exceeds this threshold, this ISV event is selected as a significant one. Based on this criterion, 74 significant ISV events are selected from these 24 yr (1979–2002), which are associated with the two ISV modes. Table 1 exhibits the start date (the rainfall anomaly begins increasing), the end date (the rainfall anomaly strops decreasing), and the duration of each significant ISV life cycle over the LYRB. The start and end dates of each event are roughly determined by the extreme dry phases of the bandpass-filtered time series of the two ISV modes. Among the 74 ISV events, 45 ISV events belong to the biweekly mode, and 29 events are

TABLE 1. The 74 significant ISV events are listed with the start dates, the begin dates, and the durations. The events associated with the biweekly mode are in bold.

ISV event No.	Start day (year-month-day)	End day (year-month-day)	Duration (day)	ISV event No.	Start day (year-month-day)	End day (year-month-day)	Duration (day)
1	1979–05–21	1979–06–14	25	**38**	1990–07–23	1990–08–20	29
2	1979–06–15	1979–07–06	22	**39**	1991–05–14	1991–06–05	23
3	1979–07–07	1979–08–01	25	**40**	**1991–06–06**	**1991–06–23**	**18**
4	1980–07–01	1980–07–23	23	**41**	1991–06–26	1991–07–18	23
5	**1980–07–24**	**1980–08–09**	**17**	**42**	1991–07–19	1991–08–15	28
6	**1981–05–16**	**1981–06–02**	**18**	**43**	**1992–06–10**	**1992–06–26**	**17**
7	**1981–06–21**	**1981–07–04**	**14**	**44**	1992–07–25	1992–08–20	27
8	**1981–07–05**	**1981–07–17**	**13**	**45**	**1992–08–09**	**1992–08–20**	**12**
9	**1981–07–19**	**1981–08–03**	**16**	**46**	**1993–05–10**	**1993–05–24**	**15**
10	**1982–05–23**	**1982–06–08**	**16**	**47**	**1993–05–25**	**1993–06–08**	**15**
11	**1982–06–13**	**1982–06–26**	**14**	**48**	**1993–06–09**	**1993–06–25**	**17**
12	1982–07–04	1982–07–27	24	**49**	**1993–06–26**	**1993–07–11**	**16**
13	**1982–08–11**	**1982–08–26**	**16**	**50**	**1994–05–05**	**1994–05–17**	**13**
14	**1983–05–09**	**1983–05–23**	**15**	**51**	1994–05–05	1994–06–02	29
15	**1983–05–24**	**1983–06–08**	**16**	**52**	1994–06–03	1994–06–26	24
16	1983–06–17	1983–07–14	28	**53**	**1994–07–08**	**1994–07–21**	**14**
17	**1983–07–15**	**1983–08–01**	**17**	**54**	**1995–05–11**	**1995–05–25**	**15**
18	1984–05–28	1984–06–23	27	**55**	**1995–05–26**	**1995–06–08**	**14**
19	1984–07–12	1984–08–05	25	**56**	1995–05–11	1995–06–08	29
20	**1985–05–09**	**1985–05–23**	**15**	**57**	**1995–06–11**	**1995–06–27**	**17**
21	**1985–06–28**	**1985–07–10**	**13**	**58**	**1996–05–30**	**1996–06–13**	**15**
22	**1986–06–08**	**1986–06–25**	**18**	**59**	1996–06–14	1996–07–07	24
23	**1986–07–10**	**1986–07–24**	**14**	**60**	**1996–07–08**	**1996–07–24**	**17**
24	1987–05–16	1987–06–10	26	**61**	**1997–06–01**	**1997–06–14**	**14**
25	**1987–06–29**	**1987–07–15**	**17**	**62**	1997–06–28	1997–07–24	27
26	**1988–04–30**	**1988–05–14**	**15**	**63**	**1998–05–05**	**1998–05–18**	**14**
27	**1988–05–15**	**1988–05–28**	**14**	**64**	**1998–06–21**	**1998–07–07**	**17**
28	1988–06–03	1988–06–25	23	**65**	1998–07–14	1998–08–06	24
29	**1988–06–14**	**1988–06–25**	**12**	**66**	**1999–05–14**	**1999–06–01**	**18**
38	**1988–07–19**	**1988–08–05**	**18**	**67**	**1999–06–20**	**1999–07–04**	**15**
31	**1988–08–13**	**1988–08–30**	**18**	**68**	2000–05–20	2000–06–14	26
32	**1989–05–30**	**1989–06–11**	**13**	**69**	**2000–06–15**	**2000–07–02**	**18**
33	**1989–06–12**	**1989–06–24**	**13**	**70**	2001–06–30	2001–07–23	24
34	1989–06–25	1989–07–18	24	**71**	2001–07–24	2001–08–19	27
35	1989–07–19	1989–08–13	26	**72**	2002–06–14	2002–07–07	24
36	**1989–07–31**	**1989–08–13**	**14**	**73**	2002–07–08	2002–08–02	26
37	**1990–06–23**	**1990–07–05**	**13**	**74**	2002–08–01	2002–08–23	23

contributed by the 21–30-day mode, which further proves that the biweekly mode is the most significant ISV mode over the LYRB during boreal summer.

To investigate how representative the ISV features derived from the LYRB are in depicting the ISV of the EA mei-yu–baiu front, we made a simultaneous correlation coefficient pattern of the rainfall intraseasonal component as shown in Fig. 2, which is calculated against the LYRB rainfall intraseasonal component over the 24 summers. We find that the precipitation ISV over the subtropical EA region, primarily including the Yangtze–Huaihe River basin, South Korea, and southern Japan, have above-significant positive correlations with that over the LYRB. Therefore, to a large extent the characteristics of the major ISV modes in the LYRB rainfall can represent the subtropical EA summer ISV.

In addition, the samples of the ISV power spectra over the LYRB in four typical summers are shown in Fig. 3. Two years (1979 and 2002) are dominated by the 21–30-day periodicity and the other two years (1981 and 1993) are dominated by the biweekly periodicity, which indicates there is large year-to-year variation of these two dominant ISV modes over the LYRB.

4. Characteristic evolutions of two major ISV modes

To obtain their genesis and evolutions of the two major empirical ISV modes, we conducted two types of statistic analysis based on daily time series of the bandpass-filtered rainfall anomalies over the LYRB (hereafter LYRB index) for each ISV mode. One is the

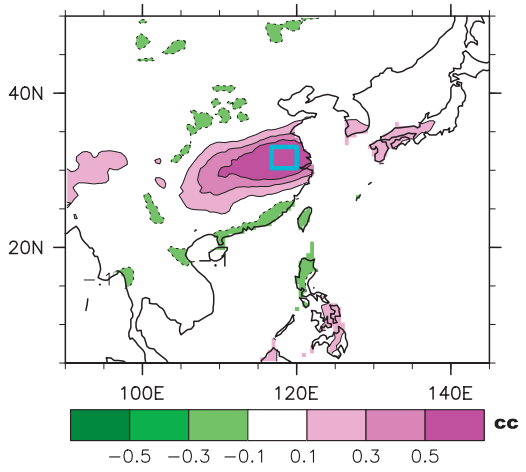

FIG. 2. Correlation coefficients (cc) between the intraseasonal rainfall at each grid and the intraseasonal component of LYRB-averaged (within the blue square) rainfall during the 24 summers (1979–2002). The regions above the 95% confidence level are shaded.

composite analysis of the strong ISV cases selected from the 24 summers (May–August) based on the LYRB index. As shown in Table 1, 45 biweekly cases and 29 cases of 21–30-day modes are chosen for their composite analysis. The other method is the point-based lead–lag correlation analysis between different meteorological fields and the maximum wet phase of the LYRB index in each ISV frequency band. Both the composite sequences and the point-based lead–lag correlation patterns demonstrate very similar life cycles for the same ISV mode. For brevity, only the results obtained from the lead–lag correlation analysis are shown below, which exhibits more smoothed contours. Day 0 is defined as the day with the maximum rainfall anomaly over the LYRB region.

a. Biweekly mode

Figures 4–5 show the half–life cycles (from day −7 to day 0) of 200-hPa vorticity and 200-hPa winds, rainfall/OLR, and 850-hPa wind anomalies, respectively, against the LYRB anomalous rainfall on the biweekly frequency band. The evolution from day −7 to day 0 completes a half-cycle because the pattern at day 0 is nearly similar to that at day −7, with reversed signs. The next life cycle is a mirror image of the presented life cycle. We notice that an anticyclonic anomaly in the upper level (Fig. 4) and a cyclonic anomaly in the low level (Fig. 5) occur over the LYRB when the maximum rainfall anomaly occurs there (day 0). This indicates that the ISV over the LYRB has a baroclinic structure, similar to the tropical ISV.

To investigate where the maximum wet phase with the baroclinic vertical structure comes from, we traced back 7 days prior to day 0 when the LYRB experiences the extreme dry phase. At day 0, the upper-level anticyclonic anomaly/negative vorticity anomaly is located over the LYRB (Fig. 4), which corresponds to the wet phase of LYRB (Fig. 5). Note that this upper-level anticyclonic anomaly can be traced back to day −7 in northern China (40°N, 120°E). This upper-level negative vorticity anomaly moves southward from 40°N to the LYRB with an increasing strength from day −7 to day 0 (Fig. 4). This southward-propagating anticyclonic anomaly is embedded in an east–west-oriented, southeastward-propagating wave train along the midlatitude westerly jet stream from the Caspian Sea to East Asia (Fig. 4). The upper-level anticyclonic anomaly tends to accompany the upper-level atmospheric divergence, which induces anomalous ascent. The enhanced upward motion not only increases the rainfall probability, but also intensifies the low-level cyclonic anomaly through enhancing the low-level convergence. Correspondingly, the southward expansion can be detected in the evolution of the rainfall anomalies (Fig. 5a).

In the lower troposphere, as shown in Fig. 5, the noticeable feature is the northwestward propagation of an anticyclonic anomaly and/or an anomalous dry area from the Philippine Sea to the south of Taiwan. The most rapid northwestward propagation occurs during the period from day −3 to day −2 when the upper-level negative vorticity anomaly arrives at the LYRB. The low-level anticyclonic anomaly over the south of Taiwan enhances the southwesterlies toward the LYRB, which not only reinforces the low-level cyclonic shear near the LYRB but also increases the wet anomaly through conveying more moisture to the LYRB region. Note also that from day −7 to day −4, the low-level midlatitude anticyclonic anomaly moves eastward (Fig. 5a), and by day −4 it moves to the Yellow Sea, while the subtropical high enhances over the Philippine Sea. At day −3 the Yellow Sea and Philippine Sea anticyclonic anomalies merge into one, further enhancing the western North Pacific subtropical high (WNPSH), and causing the Philippine Sea anticyclonic anomaly moving northwestward significantly from day −3 to day −2 (Fig. 5a). Thus, the northwestward propagation of the Philippine Sea anticyclonic anomaly, that is, the northwestward extension and the enhancement of the WNPSH, is due to a merge of a transient midlatitude high over the Yellow Sea with the subtropical high over Philippine Sea.

Initiated by the upper-level anticyclonic anomaly from the midlatitudes and enhanced by the low-level southwesterly anomaly along the southeastern China, a northeast–southwest-tilted rain belt with a baroclinic vertical structure of the circulation anomalies has been well developed from day −2 to day 0, covering the LYRB, southern Japan, and Korea.

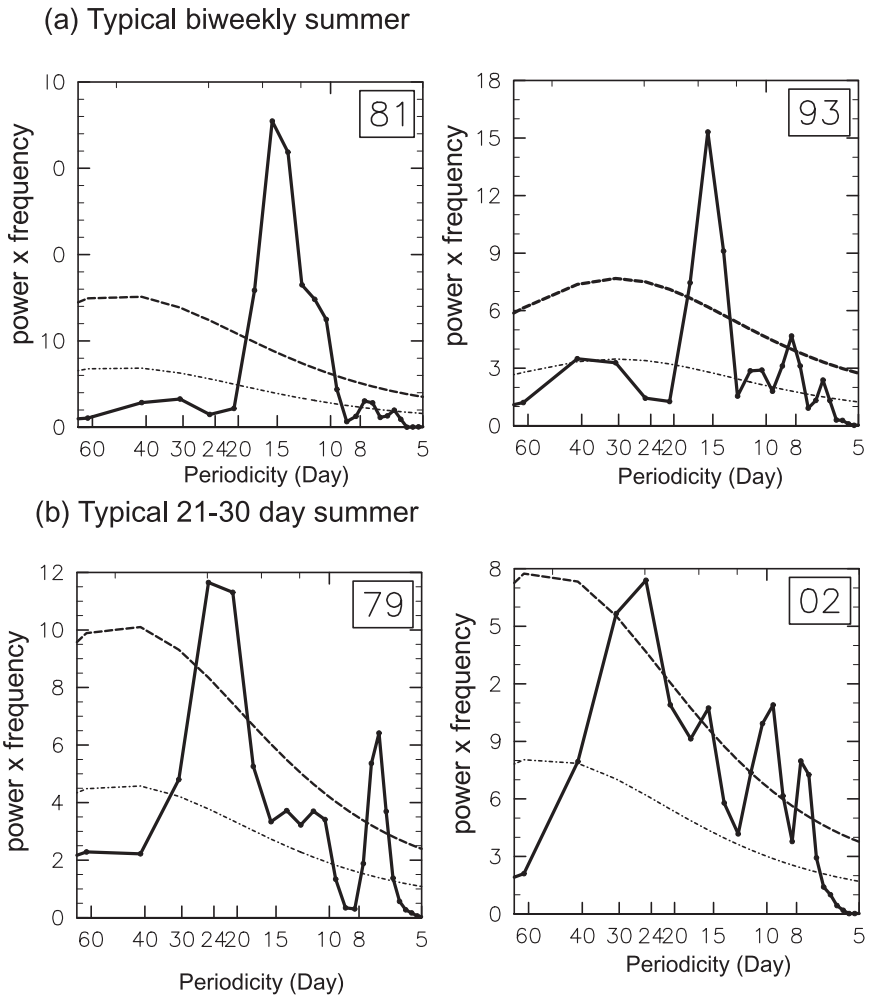

FIG. 3. Power spectra of rainfall ISV component in four individual years. The Markov red noise spectrum (dotted line) and a priori 99% confidence bound (dense dashed line). The *x* abscissa has been rescaled into the natural logarithm of the frequency, and the corresponding *y* abscissa times frequency.

b. 21–30 day

A set of time sequences similar to those for the biweekly mode are also made for the 21–30-day mode shown in Fig. 6 (and in Fig. 8 below). Additionally, the same analysis is also made for the 500-hPa geopotential height anomaly, as shown in Fig. 7. We found that the 21–30-day mode is also characterized by the out-of-phase relationship between the low- (Fig. 6) and upper-level circulations (Fig. 8; namely, the quasi-baroclinic structure) over the LYRB at day 0, which is similar to the biweekly mode. However, the genesis and evolution of the 21–30-day mode are distinct from the former mode.

According to Figs. 6a,b, the initiation and the enhancement of the wet phase over the LYRB is closely associated with a systematic westward-propagating anticyclonic anomaly from the western Pacific (145°E) to the northern SCS (120°E) along 20°N throughout the half–life cycle. This westward propagation of the low-level anticyclonic anomaly is consistent with a westward extension of 500-hPa WNPSH, which can be seen clearly in Fig. 7. As a result, the southwesterlies along the southeastern China are gradually enhanced from day −6 to day −2, which favors the genesis and the intensification of the wet phase over the LYRB through increasing the wet anomaly and the low-level cyclonic shear. In contrast to the biweekly mode, we do not find the evident contribution from the midlatitude perturbation to the westward extension of the WNPSH in Fig. 7.

In the upper-level (Fig. 8), there is no evident midlatitude migratory wave directly moving over the LYRB. However, a prominent upper-level positive vorticity

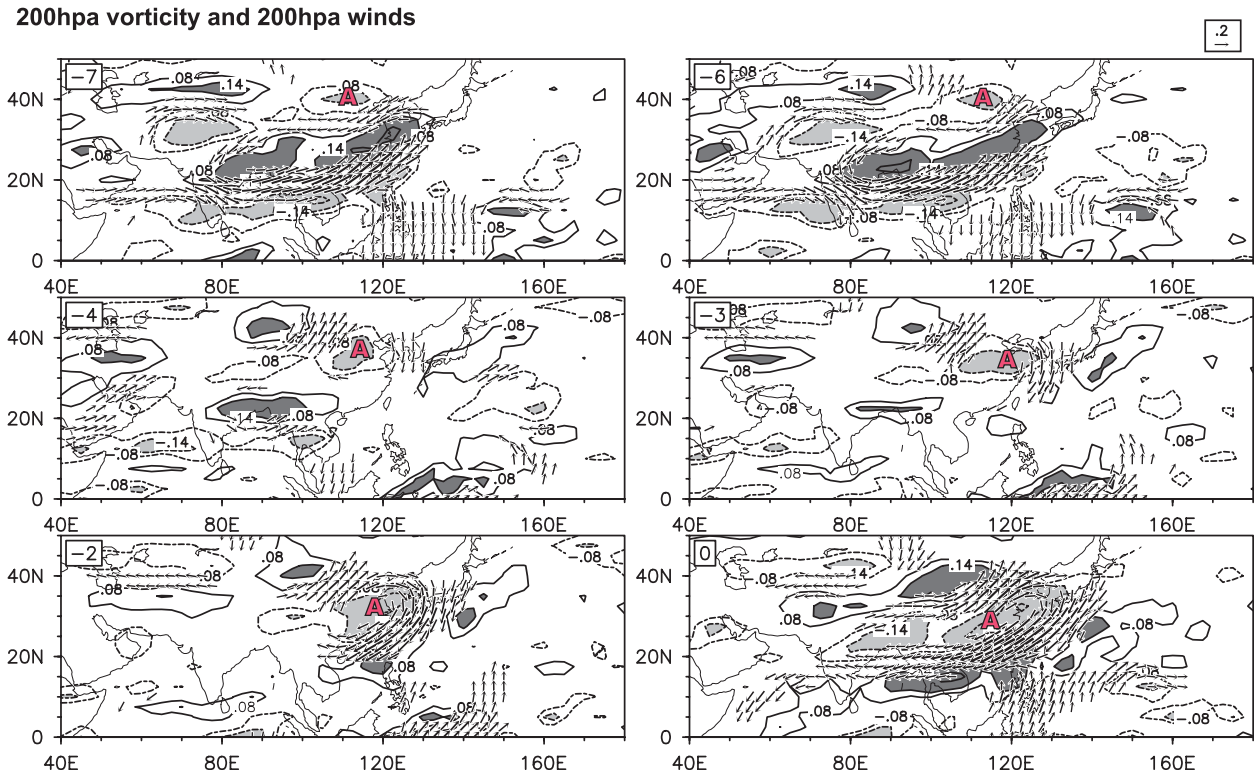

FIG. 4. Time sequences of the point-based lead correlation patterns of the filtered 200-hPa winds (with the vectors (m s^{-1}) shown above the 95% significance test) and the filtered 200-hPa vorticity anomalies (with the contours shaded above the 95% significance level and the contour interval of 0.06) in biweekly mode, which are calculated against the LYRB index in biweekly band. Solid contours represent positive vorticity anomalies while dashed contours denote negative vorticity anomalies. "A" indicates the anticyclonic anomaly.

anomaly in the higher latitudes is seen to be well established near Lake Baikal at day −8, and it moves to Far East Russia at day 0. This upper-level positive vorticity tends to deepen an upper-level trough and ahead of the anomalous upper-level trough, the low-level LYRB cyclonic vorticity is expected to be enhanced.

From day −2 to day 0, a northeast–southwest-tilted rain belt with a typical baroclinic vertical structure gets well developed, which has almost identical feature as in the biweekly mode.

5. Discussion

a. Origin of the biweekly variability over the LYRB

As depicted in the previous section, the origin of the biweekly variability over the LYRB is primarily attributed to the southeastward-propagating upper-level anticyclonic perturbations, which is embedded in east–west-oriented wave train from the Caspian Sea to East Asia. This southeastward-propagating wave train goes along the waveguide provided by the middle-latitude westerly jet, which was also depicted by Ding and Wang (2007) when they studied the intraseasonal linkage between the summer Eurasian wave train and the Indian summer monsoon. The source of this wave train is presumably associated with the northeastern Atlantic in the exit region of the Atlantic jet stream, which has been considered to be the origin of the midlatitude wave train (Simmons et al. 1983; Ding and Wang 2007). The significant biweekly periodicities are exhibited along the midlatitude westerly jet stream as shown in Fig. 9a, which indicates that the biweekly periodicity over the LYRB results from the transient perturbation with the same periodicity along the upper-level westerly jet stream. Fujinami and Yasunari (2004) has also found a well-developed wave train along the Asian subtropical jet associated with the submonthly (7–20-day) convective fluctuations over the plateau, which is almost consistent with what we found in this study.

The development of the biweekly extreme wet phase over the LYRB is also enhanced by the northwestward-propagating anticyclonic anomaly from the Philippine Sea to the northern SCS (Fig. 5), which is consistent with the enhancement and the westward extension of the WNPSH. That means that the midlatitude perturbation forcing is important for the enhancement of the

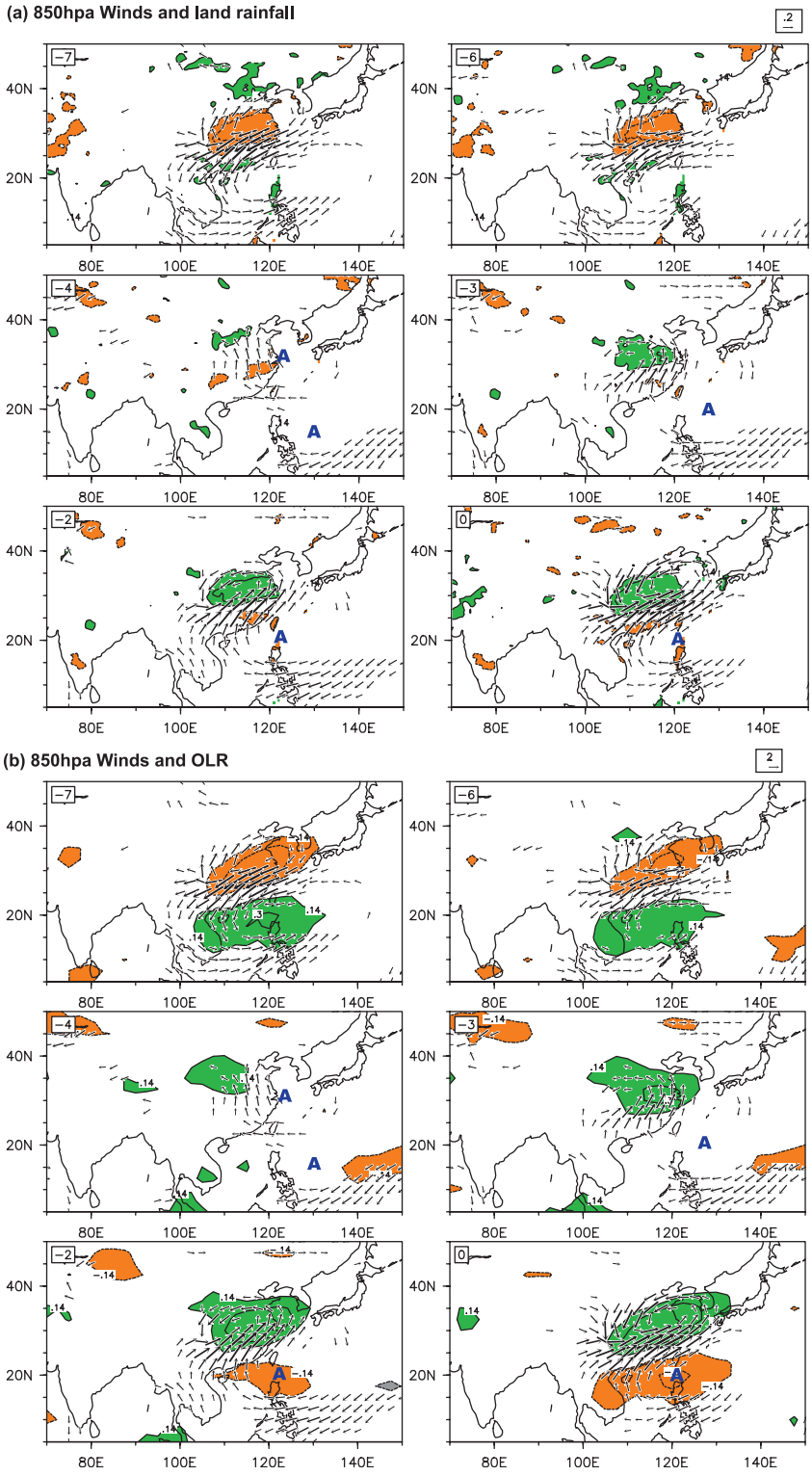

FIG. 5. (a) Time sequences of the point-based lead correlation patterns of the 850-hPa winds [with vectors (m s^{-1}) shown above the 95% significance level] and the rainfall anomalies (with contours shaded above the 95% significance level) in the biweekly modes, which are both calculated against the biweekly LYRB index. The minimum value of contour is 0.14 and the contour interval is 0.06. The green shading is for the wet anomaly and the orange is for the dry anomaly. "A" denotes the anticyclonic anomaly. (b) As in (a), but with the OLR anomalies.

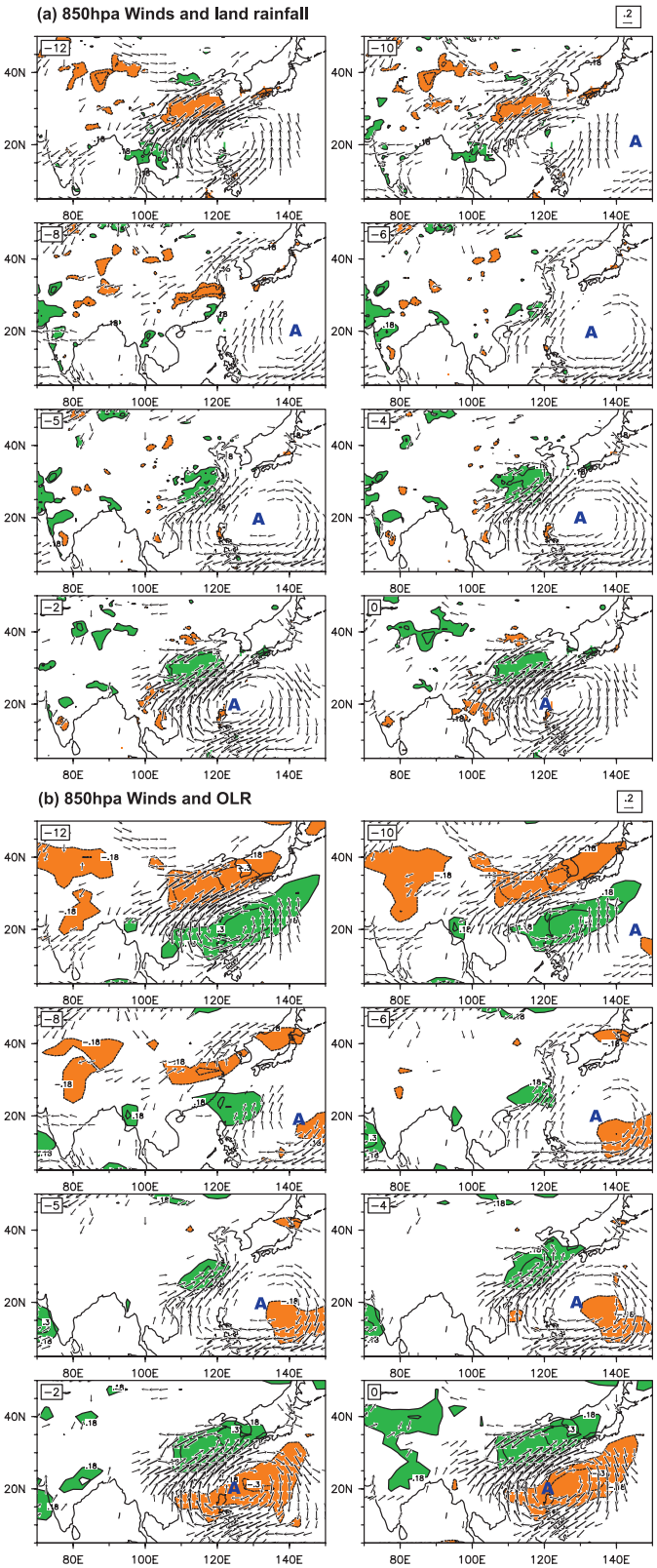

FIG. 6. (a) As in Fig. 5a, but for the 21–30-day mode; "C" represents the cyclonic anomaly. The minimum value of contour is 0.18 and the contour interval is 0.12. (b) As in Fig. 5b, but for the 21–30-day mode.

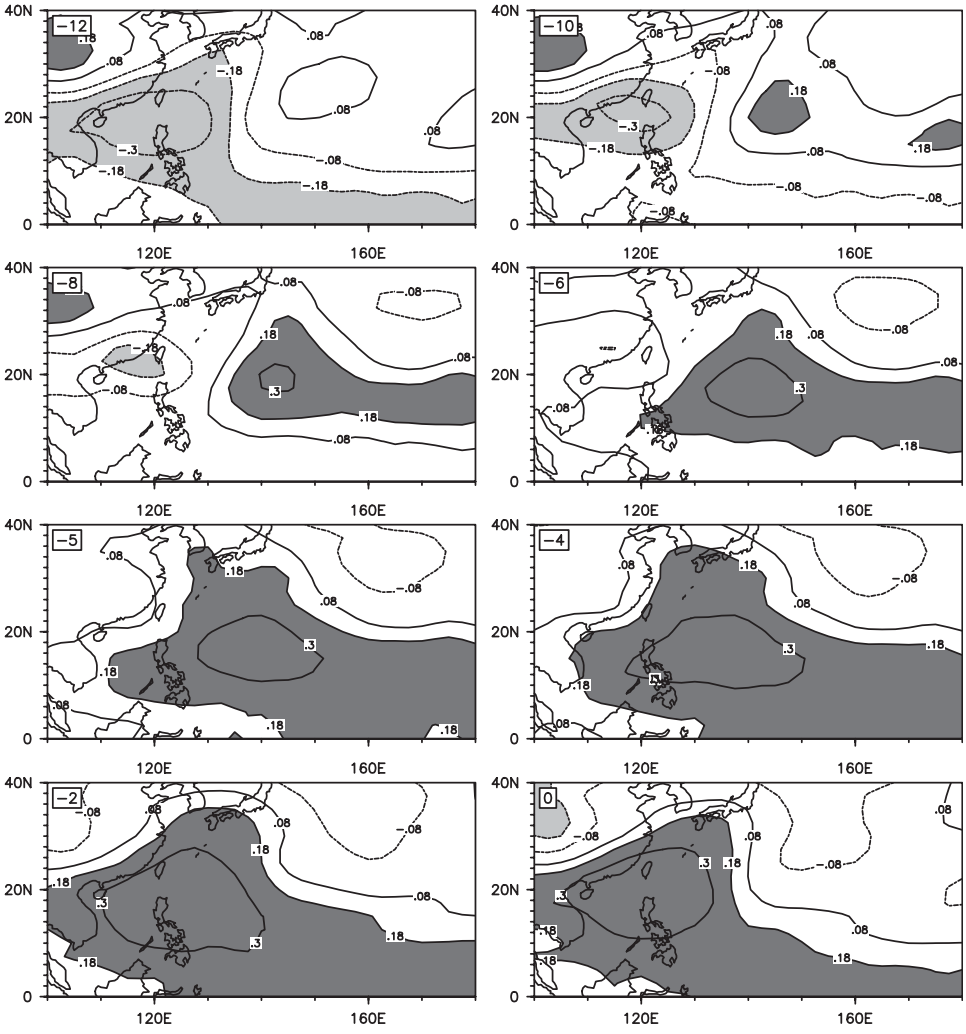

FIG. 7. Time sequences of the point-based lead correlation patterns of the filtered 500-hPa vorticity anomalies (with the contours shaded above the 95% significance level) in 21–30-day mode, which are calculated against the LYRB index in 21–30-day band.

subtropical high on this time scale. The westward propagation from the Philippine Sea to the South China Sea in the biweekly time scale has been widely explored in previous literature (Annamalai and Slingo 2001; Mao and Chan 2005; Yang et al. 2008; Kikuchi and Wang 2009). However, the origin of the biweekly mode over the western Pacific has not been clarified yet. The linkage between the midlatitude disturbance and the westward extension of WNPSH in the biweekly mode indicates that the biweekly mode over the western Pacific may be associated with the WNPSH intraseasonal activity, and its origin could be attributed to the midlatitude perturbation.

b. Origin of the 21–30-day variability over the LYRB

In contrast to the biweekly mode, the extreme wet phase of the 21–30-day mode over the LYRB is mainly initiated by the westward-propagating low-level anticyclonic anomaly from the western Pacific to the northern SCS–Philippine Sea. This westward-propagating low-level anticyclonic anomaly is evidently linked with the westward extension of the WNPSH. We made a multiyear-averaged power spectrum of OLR over the western Pacific (15°–25°N, 125°–135°E), as shown in Fig. 9b, which exhibits a significant peak around days 21–30. In addition, a 20–30-day period has been found over the Philippine Sea–western North Pacific in previous studies characterized with the westward propagation at about 10°–20°N (e.g., Murakami 1980). The 20–30-day westward-propagating mode has been found also to be one of the dominant intraseasonal modes of WNPSH activities in several previous studies (e.g., Tao et al. 2001; Zhang et al. 2003). Therefore, the origin of the 21–30-day mode

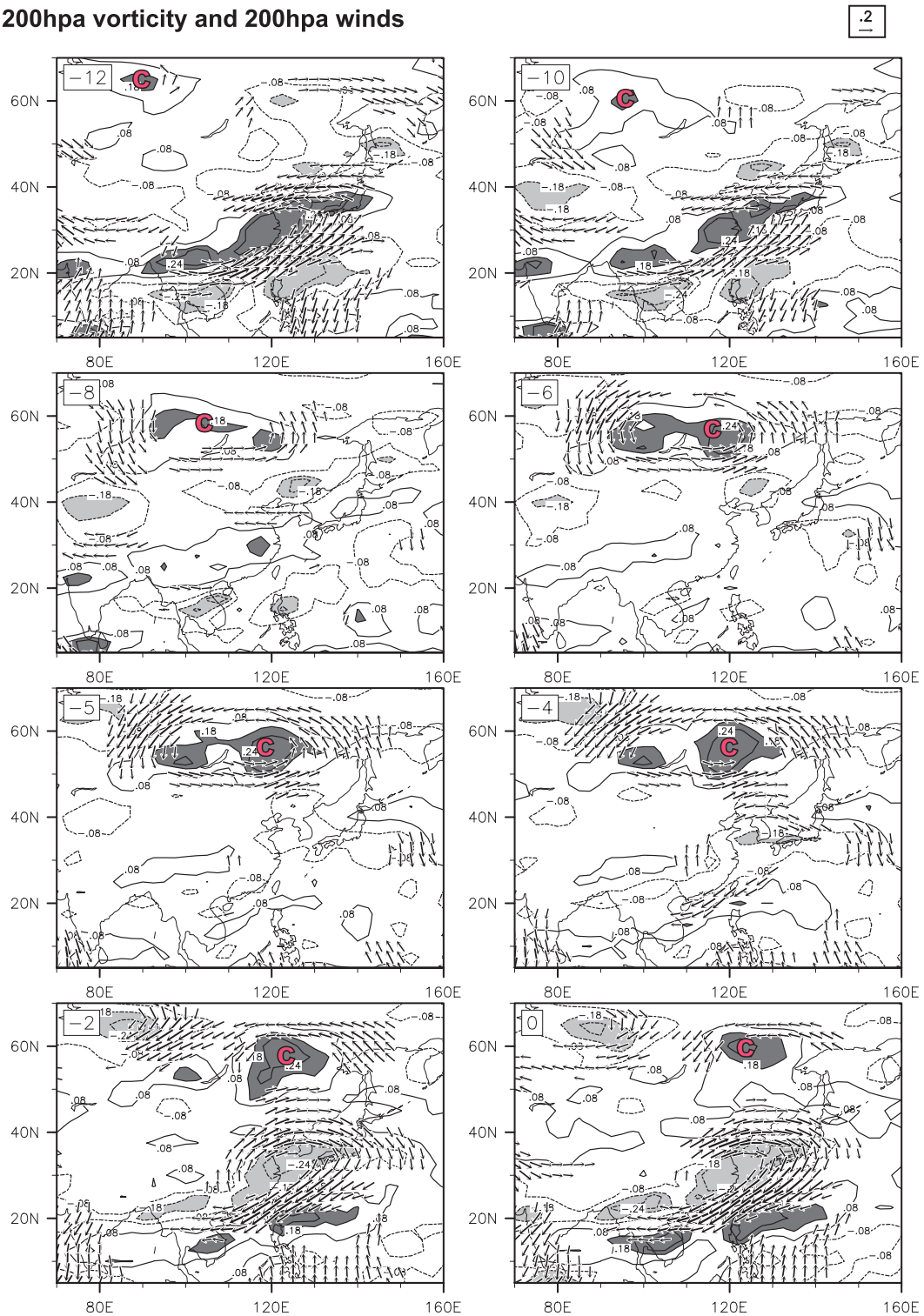

FIG. 8. As in Fig. 4, but for the 21–30-day mode.

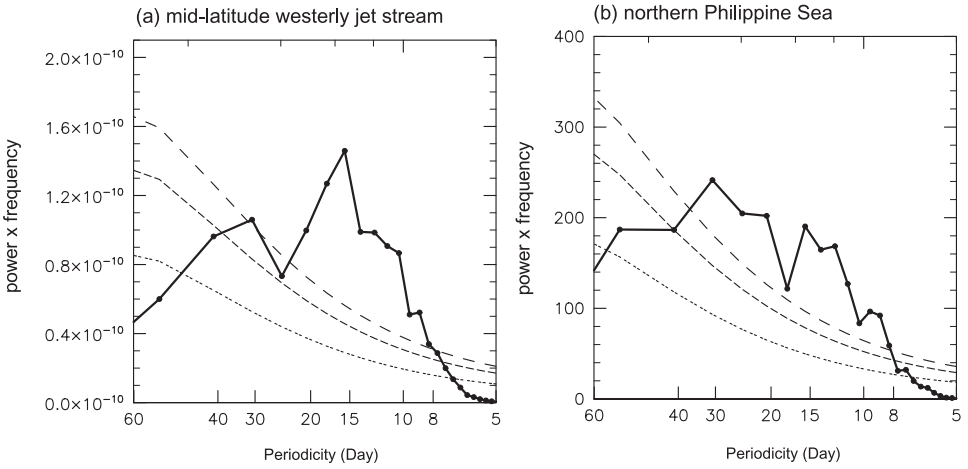

FIG. 9. The mean power spectra calculated in the same way as in Fig. 1, but for (a) the 200-hPa vorticity near the midlatitude westerly jet stream (35°–45°N, 90°–120°E), and (b) the OLR over the western Pacific (15°–25°N, 125°–135°E).

over the LYRB is mostly connected with the intraseasonal activity of WNPSH, which is different from the biweekly mode that is more associated with the midlatitude perturbations.

6. Summary

The LYRB is a central region over the subtropical EA monsoon. Based on newly released daily rainfall data with a high resolution (0.5° × 0.5°) and long record (1979–2002), two major empirical ISV modes are identified from 24-yr mean spectra of the summer precipitation over the LYRB, respectively, on biweekly and 21–30-day time scales. These two ISV modes together contribute around 57% variance to the total ISV over the LYRB. The biweekly mode is the most dominant ISV mode over the LYRB.

These two ISV modes share some common features, including that both are characterized by the baroclinic vertical structures over the LYRB at their extreme phases and both of their developments are associated with the westward extension of the WNPSH. However, both their origins and their evolutions are different, which are summarized in a schematic diagram (Fig. 10). 1) They have different origins: the wet phases of the biweekly mode is primarily induced by an upper-level anticyclonic anomaly, which is embedded in the southeastward-propagating wave train along the midlatitude westerly jet stream; whereas the wet phase of the 21–30-day mode is initiated by the low-level anticyclonic anomaly moving westward from the western Pacific (145°E) to the northern SCS (120°E), which is associated with a evident westward extension of the WNPSH. Furthermore, the spectrum analysis indicates that the source of the biweekly periodicity comes from the midlatitude jet stream perturbation, while the 21–30-day periodicity primarily originates from the western Pacific and is directly linked with the WNPSH intraseasonal activity. 2) They have different evolutions: the development of the biweekly wet phase over the LYRB is enhanced by the northwestward propagation of low-level anticyclonic anomaly from Philippine Sea to south of Taiwan, which is a result of the enhancement of the WNPSH resulting from a merger of the original WNPSH with a midlatitude high anomaly. In contrast, the development of the 21–30-day wet phase over the LYRB is associated with an upper-level trough moving from Lake Baikal to far east Russia, which possibly enhances the low-level LYRB low-level cyclonic vorticity.

The identification of the two ISV modes over the LYRB and the new knowledge on their sources and evolution provide empirical predictors for the local intraseasonal variation in the subtropical EA summer monsoon. Although, the primary features of the two ISV modes have been addressed in this study, the detailed mechanism for the selection of the periodicities in their source regions is still an interesting question to be answered: that is, how is the 21–30-day variation associated with the WNPSH generated? Why is there a strong biweekly signal along the middle-latitude westerly jet stream? Is the biweekly mode over the western Pacific only attributed by the midlatitude perturbation, or are there any other factors? In addition, the intensities of the two ISV modes experience the large year-to-year variation over the LYRB, but what controls the year-to-year variations of the dominant periodicity over this region calls for further studies.

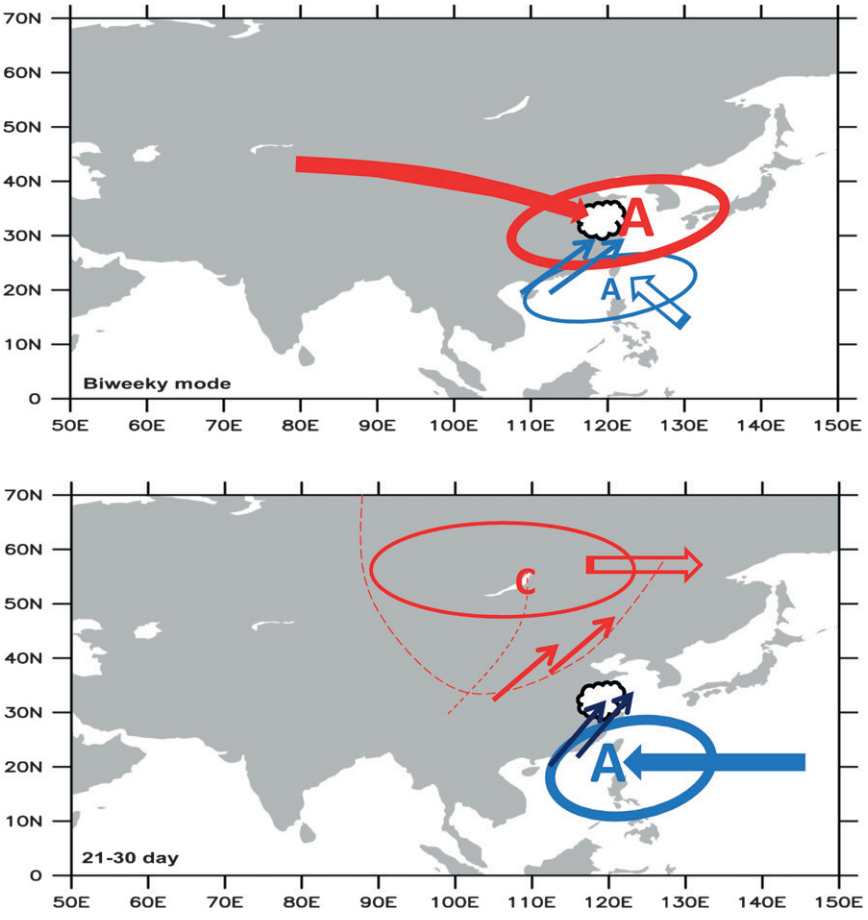

FIG. 10. A schematic diagram to summarize the difference between the genesis and evolution of the wet phases associated with the two ISV modes over the LYRB: biweekly and (bottom) 21–30 day mode. The primary disturbances contributing to the initiation of each ISV mode are highlighted with bold. "A" and "C" respectively represent the anticyclonic and cyclonic anomalies. The red and blue colors respectively denote the upper- and the low-level disturbances. The thick solid blank arrows portray the propagating routines of these perturbations, and the thin arrows represent the winds.

Acknowledgments. The authors would like to show their thanks to Dr. Kajikawa for the information of the land precipitation data and his constructive discussion in the initial stage of this work. Jing Yang acknowledges the financial support from the Knowledge Innovation Program of the Chinese Academy of Sciences (KZCX2-YW-Q11-04) and State Key Laboratory of Earth Surface Processes in Beijing Normal University (Grant 070205); Bin Wang at University of Hawaii acknowledges the support received from NSF Award ATM-0647995; Bin Wang in LASG is supported by NSFC (Grant 40821092); Qing Bao is supported by the NSFC (Grant 40805038).

REFERENCES

Annamalai, H., and J. M. Slingo, 2001: Active/break cycles: Diagnosis of the intraseasonal variability of the Asian Summer Monsoon. *Climate Dyn.,* **18,** 85–102.

Bingham, C., M. D. Godfrey, and J. W. Tukey, 1967: Modern techniques of power spectrum estimation. *IEEE Trans. Audio Electroacoust.,* **AU-15,** 56–66.

Chao, J. M., 1991: The characteristics of the quasi-two week oscillation of isobaric surface geopotential height over China and its relationships with the summer monsoon strength and the rainfall over the northern China from July to August (in Chinese). *Acta Geogr. Sin.,* **4,** 23–30.

Chen, T. C., and M. Murakami, 1988: The 30–50 day variation of convective activity over the western Pacific Ocean with emphasis on the northwestern region. *Mon. Wea. Rev.,* **116,** 892–906.

——, and J. R. Chen, 1995: An observational study of the South China Sea monsoon during the 1979 summer: Onset and life cycle. *Mon. Wea. Rev.,* **123,** 2295–2318.

——, M. C. Yen, and S. P. Weng, 2000: Interaction between the summer monsoons in East Asia and the South China Sea: Intraseasonal monsoon modes. *J. Atmos. Sci.,* **57,** 1373–1392.

Chen, W. Y., 1982: Fluctuations in Northern Hemisphere 700 mb height field associated with Southern Oscillation. *Mon. Wea. Rev.,* **110,** 808–883.

Ding, Q., and B. Wang, 2007: Intraseasonal teleconnection between the Eurasian wave train and Indian monsoon. *J. Climate,* **20,** 3751–3767.

Ding, Y. H., 1992: Summer monsoon rainfall in China. *J. Meteor. Soc. Japan,* **70,** 373–396.

Fujinami, H., and T. Yasunari, 2004: Submonthly variability of convection and circulation over and around the Tibetan Plateau during the boreal summer. *J. Meteor. Soc. Japan,* **82,** 1545–1564.

Gilman, D. L., F. J. Fuglister, and J. M. Mitchell Jr., 1963: On the power spectrum of red noise. *J. Atmos. Sci.,* **20,** 182–184.

Hsu, H. H., and C. H. Weng, 2001: Northwestward propagation of the intraseasonal oscillation in the western North Pacific during the boreal summer: Structure and mechanism. *J. Climate,* **14,** 3834–3850.

——, C.-H. Weng, and C.-H. Wu, 2004: Contrasting characteristics between the northward and eastward propagation of the intraseasonal oscillation during the boreal summer. *J. Climate,* **17,** 727–743.

Kajikawa, Y., and T. Yasunari, 2005: Interannual variability of the 10–25- and 30–60-day variation over the South China Sea during boreal summer. *Geophys. Res. Lett.,* **32,** L04710, doi:10.1029/2004GL021836.

Kanamitsu, M., W. Ebisuzaki, J. Woollen, S. K. Yang, J. J. Hnilo, M. Fiorino, and G. L. Potter, 2002: NCEP-DOE AMPI-II Reanalysis (R-2). *Bull. Amer. Meteor. Soc.,* **83,** 1631–1643.

Kang, I. S., C. H. Ho, Y. K. Lim, and K. M. Lau, 1999: Principal modes of climatological seasonal and intraseasonal variations of the Asian summer monsoon. *Mon. Wea. Rev.,* **127,** 322–340.

Kemball-Cook, S., and B. Wang, 2001: Equatorial waves and air–sea interaction in the boreal summer intraseasonal oscillation. *J. Climate,* **14,** 2923–2942.

Kikuchi, K., and B. Wang, 2009: Global perspectives of the quasi-biweekly oscillation. *J. Climate,* **22,** 1340–1359.

Krishnamurti, T. N., and H. N. Bhalme, 1976: Oscillations of a monsoon system. Part I: Observational aspects. *J. Atmos. Sci.,* **33,** 1937–1954.

——, and P. Ardanuy, 1980: The 10 to 20 day westward propagating modes and breaks in the monsoons. *Tellus,* **32,** 15–26.

——, and D. Subrahmanyam, 1982: The 30-50 day mode at 850 mb during MONEX. *J. Atmos. Sci.,* **39,** 2088–2095.

Lau, K.-M., G. J. Yang, and S. H. Shen, 1988: Seasonal and intraseasonal climatology of summer monsoon rain over East Asia. *Mon. Wea. Rev.,* **116,** 18–37.

Lawrence, D. M., and P. J. Webster, 2002: The boreal summer intraseasonal oscillation: Relationship between northward and eastward movement of convection. *J. Atmos. Sci.,* **59,** 1593–1606.

Liebmann, B., and C. A. Smith, 1996: Description of a complete (interpolated) outgoing longwave radiation dataset. *Bull. Amer. Meteor. Soc.,* **77,** 1275–1277.

LinHo, and B. Wang, 2002: The time-space structure of the Asian-Pacific summer monsoon: A fast annual cycle view. *J. Climate,* **15,** 2001–2019.

Liu, H., D.-L. Zhang, and B. Wang, 2008: Daily to submonthly weather and climate characteristics of the summer 1998 extreme rainfall over the Yangtze River Basin. *J. Geophys. Res.,* **113,** D22101, doi:10.1029/2008JD010072.

Liu, J., B. Wang, and J. Yang, 2008: Forced and internal modes of variability of the East Asian summer monsoon. *Climate Past,* **4,** 1–9.

Livezey, R. E., and W.-Y. Chen, 1983: Statistical field significance and its determination by Monte Carlo techniques. *Mon. Wea. Rev.,* **111,** 46–59.

Mao, J. Y., and J. C. L. Chan, 2005: Intraseasonal variability of the South China Sea summer monsoon. *J. Climate,* **18,** 2388–2402.

——, and G. X. Wu, 2006: Intraseasonal variations of the Yangtze rainfall and its related atmospheric circulation features during the 1991 summer. *Climate Dyn.,* **27,** 815–830.

Murakami, T., 1980: Empirical orthogonal function analysis of satellite-observed outgoing longwave radiation during summer. *Mon. Wea. Rev.,* **108,** 205–222.

Nakazawa, T., 1992: Seasonal phase lock of intraseasonal variation during the Asian summer monsoon. *J. Meteor. Soc. Japan,* **70,** 597–611.

Onogi, K., and Coauthors, 2007: The JRA-25 Reanalysis. *J. Meteor. Soc. Japan,* **85,** 369–432.

Simmons, A. J., J. M. Wallace, and G. W. Branstator, 1983: Barotropic wave propagation and instability, and atmospheric teleconnection patterns. *J. Atmos. Sci.,* **40,** 1363–1392.

Tao, S.-Y., and L. S. Chen, 1987: A review of recent research on the East Asian summer monsoon in China. *Monsoon Meteorology,* C. P. Chang and T. N. Krishnamurti, Eds., Oxford University Press, 60–92.

——, Q. Zhang, and S. Zhang, 2001: An observational study on the behavior of the subtropical high over the west Pacific in summer. *Acta Meteor. Sin.,* **59,** 748–758.

Uppala, S. M., and Coauthors, 2005: The ERA-40 Re-Analysis. *Quart. J. Roy. Meteor. Soc.,* **131,** 2961–3012.

Wang, B., and X. H. Xu, 1997: Northern Hemisphere summer monsoon singularities and climatological intraseasonal oscillation. *J. Climate,* **10,** 1071–1085.

Wang, Y., O. L. Sen, and B. Wang, 2003: A highly resolved regional climate model (IPRC RegCM) and its simulation of the 1998 severe precipitation event over China. Part I: Model description and verification of simulation. *J. Climate,* **16,** 1721–1738.

Wilks, D. S., 1995: *Statistical Methods in the Atmospheric Sciences: An Introduction*. Academic Press, 467 pp.

Xie, P., A. Yatagai, M. Chen, T. Hayasaka, Y. Fukushima, C. Liu, and S. Yang, 2007: A gauge-based analysis of daily precipitation over East Asia. *J. Hydrometeor.,* **8,** 607–627.

Yang, J., 2008: Climatological and transient intraseasonal oscillations in the East-Asia-Western North Pacific summer monsoon. Ph.D. dissertation, Insititute of Atmospheric Physics, Chinese Academy of Sciences, 106 pp.

——, B. Wang, and B. Wang, 2008: Anticorrelated intensity change of the quasi-biweekly and 30–50-day oscillations over the South China Sea. *Geophys. Res. Lett.,* **35,** L16702, doi:10.1029/2008GL034449.

Yatagai, A., P. Xie, and P. Alpert, 2008: Development of a daily gridded precipitation data set for the Middle East. *Adv. Geosci.,* **12,** 165–170.

Zhang, Q. Y., S. Y. Tao, and S. L. Zhang, 2003: The persistent heavy rainfall over the Yangtze River valley and its associations with the circulations over East Asia during summer (in Chinese). *Chinese J. Atmos. Sci.,* **27,** 1018–1030.

Zhang, X. L., P. W. Guo, and J. H. He, 2002: Characteristics of low frequency oscillation of precipitation and wind field in the middle and low reaches of the Yangtze River in summer 1991 (in Chinese). *J. Nanjing Inst. Meteor.,* **25,** 388–394.

Zhu, C. W., T. Nakazawa, J. Li, and L. Chen, 2003: The 30–60 day intraseasonal oscillation over the western North Pacific Ocean and its impacts on summer flooding in China during 1998. *Geophys. Res. Lett.,* **30,** 1952, doi:10.1029/2003GL017817.